paper CD-4: 1991
Cryogenic Engineering
Conference. Huntsville, AL

51-34
46266

N92-11295

CHARACTERIZING HE II FLOW THROUGH POROUS MATERIALS USING COUNTERFLOW DATA

J. R. Maddocks and S. W. Van Sciver,

University of Wisconsin, Madison,
Applied Superconductivity Center,
Madison, Wisconsin

ABSTRACT

Proposed space applications, such as the cooling of infrared and x-ray telescopes, have generated substantial interest in the behavior of He II flowing in porous materials. For design purposes, classical porous media correlations and room temperature data are often used to obtain order of magnitude estimates of expected pressure drops, while the attendant temperature differences are either ignored or estimated using smooth tube correlations. A more accurate alternative to this precedure is suggested by an empirical extension of the two fluid model. It is shown that four empirical parameters are necessary to describe the pressure and temperature differences induced by He II flow through a porous sample. The three parameters required to determine pressure differences are measured in counterflow and found to compare favorably with those for isothermal flow. The fourth parameter, the Gorter-Mellink constant, differs substantially from smooth tube values. It is concluded that parameter values determined from counterflow can be used to predict pressure and temperature differences in a variety of flows to an accuracy of about ±20%.

INTRODUCTION

A general interest in the behavior of He II flowing through porous materials stems from recent space based technological applications, which require the management of He II in a weightless environment. Specific applications include; fine mesh screens and light weight, high porosity ceramics for fluid acquisition devices,[1] sintered metal or packed metal powders for use as porous venting plugs[2,3] and very fine pore packed powders or ceramics to be used as superleaks.[4,5]

For design purposes, the Darcy permeability of a specific porous sample, measured at room temperature, is often used to obtain order of magnitude estimates of expected pressure drops. Expected temperature differences are either neglected or estimated using the Gorter-Mellink relation and smooth tube values of the Gorter-Mellink parameter. However, experiments show that the major portion of the pressure drop

in high porosity ceramics results from kinetic energy losses rather than viscous drag losses due to laminar flow. In addition, the superfluid losses are not generally negligable. The result is that room temperature measurements of the permeability do not provide adequate pressure loss estimates.

Through a set of experiments discussed in the present paper we show that a better method of characterizing porous media for He II applications involves a straightforward measurement of counterflow heat transport. These results combined with knowledge of the porous media appear to allow the prediction of temperature and pressure gradients through the medium to within ± 20%.

GOVERNING EQUATIONS

The equations most commonly used to analyze the behavior of He II in simple one dimensional geometries are:

$$\rho_s (Dv_s/Dt) = -\nabla P_s - F_s - F_{sn}, \tag{1}$$

and

$$\rho_n (Dv_n/Dt) = -\nabla P_n + \eta_n \nabla^2 v_n - F_n + F_{sn}, \tag{2}$$

where

$$\nabla P_s = (\rho_s/\rho)\nabla P - \rho_s s \nabla T, \tag{3}$$

$$\nabla P_n = (\rho_n/\rho)\nabla P + \rho_s s \nabla T. \tag{4}$$

The empirical forces F_n, F_s and F_{sn} are added to account for the effects of normal fluid turbulence, superfluid turbulence and mutual friction respectively.

To formulate the equations of motion in a way that is applicable to porous materials, the following functional forms are assumed. Based on a previous experiment[6] it is assumed that,

$$F_n = b_n \rho_n v_n^2, \tag{5}$$

$$F_s = b_s \rho_s v_s^2. \tag{6}$$

It is further assumed that the Gorter-Mellink relationship describes the mutual friction, so that

$$F_{sn} = A(T)\rho_s \rho_n (v_s - v_n)^3. \tag{7}$$

Finally, the empirical Darcy law,

$$\nabla P = -\eta(v/k), \tag{8}$$

is used to replace the laminar term ($\eta_n \nabla^2 v_n$) in equation (2), where k is the Darcy permeability.

Each term in equations (1) and (2) is replaced by its appropriate functional form. Steady state conditions are assumed, so the time derivatives are set equal to zero, and the equations then reduce to:

$$\nabla P_s = -b_s \rho_s v_s^2 - A(T)\rho_s\rho_n(v_s - v_n)^3 \quad (9)$$

$$\nabla P_n = -(\eta_n/k)v_n - b_n\rho_n v_n^2 + A(T)\rho_s\rho_n(v_s - v_n)^3. \quad (10)$$

The present experiment is designed to test the appropriatness of this empirical model.

MATERIALS, APPARATUS AND PROCEDURE

The porous material used in the present experiment is a fibrous ceramic of the type used for heat shields on the space shuttle. The fibers consist of 78% silica and 22% aluminum borosilicate. The material is manufactured by Lockheed,[7] using a process which results in an inhomogeneous and anisotropic final product. It is available in a number of packing densities. Samples of 6 and 16 lbs/ft^3 are tested in the present experiment. The porosity (ε) of each sample type, determined as $\varepsilon = 1 - (\rho_{sample}/\rho_{fiber})$, is listed in Table 1.

The test section, shown schematically in figure 1, contains two symmetrically mounted samples separated by approximately 10 mm. It is configured as such to allow a broader study including isothermal flow and combined flow.[8] Within the test section, the samples are mounted in thin wall stainless steel tubing, to minimize parallel heat conduction paths. Heat conduction through the ceramic samples may be neglected, because the thermal conductivity of the sample material is at least six orders of magnitude smaller than that of He II. To insure that the samples fit tightly, they are carefully cut using a sharpened piece of the same stainless tubing in which they are mounted. The outer surface of the samples is lightly covered with vacuum grease, to ensure their ridgid placement duing experimentation. The room temperature permeabilities of several samples are carefully measured using helium gas, and two closely matched samples are selected and mounted in the test section.

A 110 Ω metal film resistor serves as a heater and is located between the samples. Allen-Bradley carbon resistors serve as thermometers. As indicated in figure 1, there are three thermometers, each located in the liquid. One between the samples and one approximately 2 mm outside each sample. They provide an absolute temperature resolution of ±0.5 mK. Temperature differences across the samples are determined by subtracting the absolute temperatures measured on either side of the samples. Finally, pressure drops across each sample are measured

Table 1. Comparison of the permeability and the coefficient b_n

sample	porosity	k_{gas}	k_{iso}	k_{cf}	$(b_n)_{iso}$	$(b_n)_{cf}$
		$m^2 \times 10^{11}$			m^{-1}	
6#	.96	5.7	22	8.5	8600	7300
16#	.90	2.9	10	3.5	13200	11500

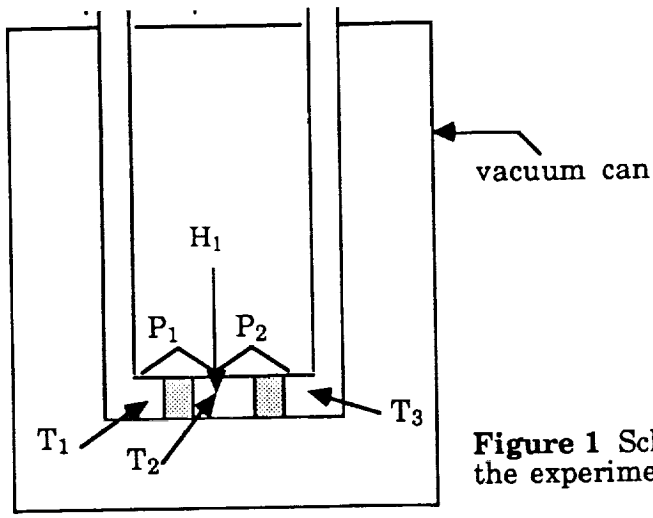

Figure 1 Schematic representation of the experimental apparatus.

using Siemens KPY-33R pressure sensors. These sensors have a nominal full scale range of 10 kPa and are mounted differentially. Their resolution is ±1 Pa.

All data are taken in the steady state with the aid of a Masscomp computer and associated periferals. The two pressure sensors, and the bath temperature are sampled sequentially at a burst rate of 1 MHz. This sequential sampling is repeated 25 times per second, for 32 seconds. The digitized data are then averaged to give a steady-state value.

During a somewhat longer but overlapping time period, the carbon resistance thermometers are sampled. The thermometers are sampled in sequence, each for a period of 10 seconds, at a sampling frequency of 6 Hz. This sampling frequency is determined by an A.C. conductance bridge, which is used to read the output of the thermometers. The bridge is a null device that gives a four-wire measurement of the conductance, by providing a 300 mV, 24 Hz excitation voltage.

EXPERIMENTAL RESULTS

For the purpose of data analysis, it is assumed that any effects due to mismatched samples can be neglected, so that half the heat deposited between the samples flows through each sample. Thus the relation

$$v_n = q/(2\rho s T A \varepsilon) \tag{11}$$

is used to determine v_n, where q is the total heat deposited, A the cross sectional area and ε the porosity.

While it is expected that this assumption will not cause a great deal of error in the analysis, it means that small differences in permeability (k), b_n, b_s and A(T) will not be measureable, as a result of the fixed boundary conditions.

A pressure gradient is always observed to accompany the flow of heat through He II in a narrow channel or porous material. The expected form of the pressure drop is given by the sum of equations (9), and (10) as

$$\nabla P = -(\eta/k)v_n - [b_n - (\rho_n/\rho_s)b_s]\,\rho_n v_n^2, \tag{12}$$

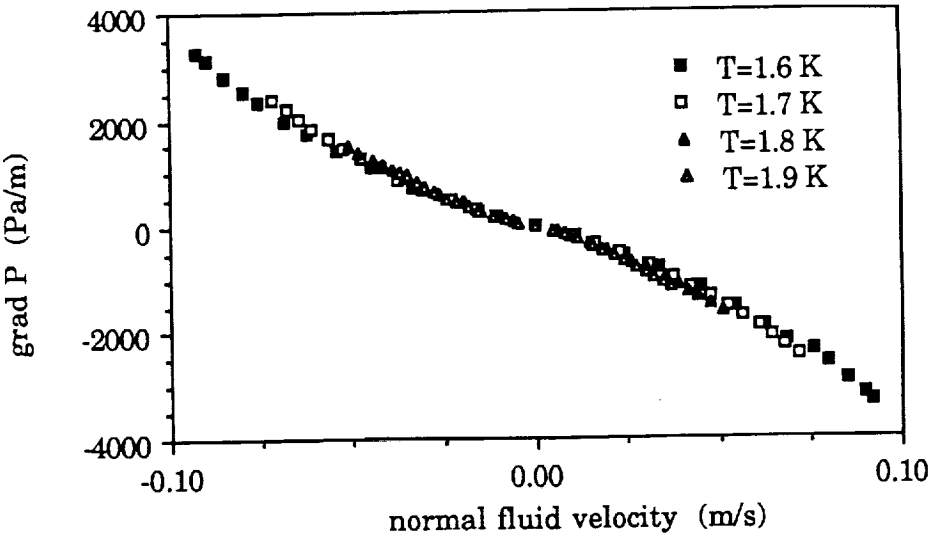

Figure 2 Velocity dependence of the pressure gradient, as a function of the temperature, for the 6# samples.

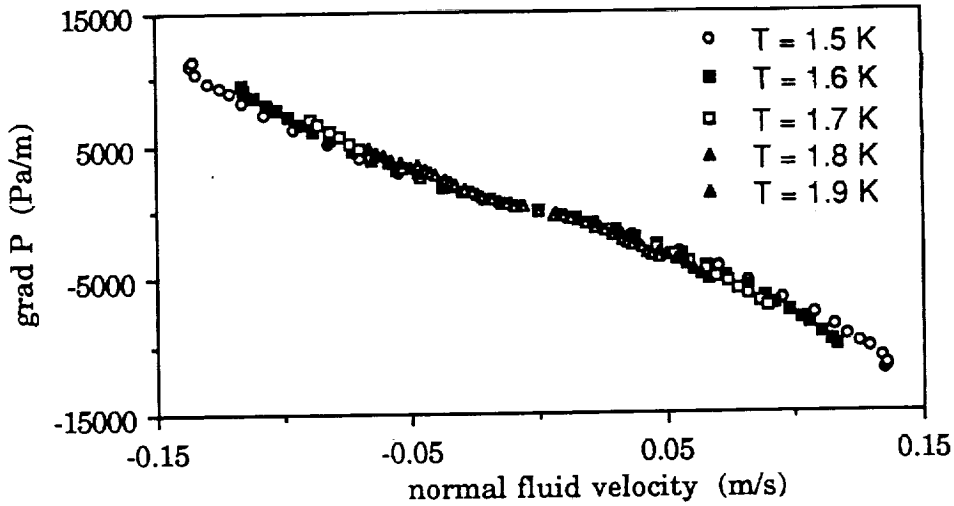

Figure 3 Velocity dependence of the pressure gradient, as a function of the temperature, for the 16# samples.

where the counterflow condition, $v_s = -(\rho_n/\rho_s)v_n$, has been used.

Figures 2 and 3 are plots of pressure gradient versus normal fluid velocity for the 6# and 16# samples. It is evident in both figures that the linear relationship between ∇P and v_n breaks down at normal velocities in excess of approximately 10 mm/s. This shows that the Allen and Reekie rule does not apply, even if modified to use the Darcy law for porous materials. In addition, the pressure gradients in figures 2 and 3 exhibit a small but definite temperature dependence. In order to determine if this temperature dependence is predictable, equation (12) is rewritten in the form

$$\nabla P/v_n = -\alpha(T) - \beta(T)v_n \qquad (13)$$

where, $\alpha(T) \equiv \eta/k$ and $\beta(T) \equiv \{b_n - (\rho_n/\rho_s)b_s\}\,\rho_n$.

Theoretically, the permeability can be determined from a plot of $\alpha(T)$ versus η_n. Practically, however, there is a large amount of scatter in $\alpha(T)$ because the pressure drop at low velocities, where laminar flow dominates, is not much larger than experimental resolution. Therefore, the permeability is determined using average values of $\alpha(T)$ and η_n. The permeabilities measured in this fashion are recorded in Table 1 and agree reasonably well with those measured in room temperature gas flow experiments. Agreement with isothermal permeabilities is not as good, but this may be due to the method used to obtain isothermal flow.[8]

In figure 4, the temperature dependence of the quadratic term, $\beta(T)$, is compared to that predicted by equation (12). The figure shows little sign of the expected temperature dependence, though clearly, $\beta(T)$ is affected by temperature. A plot of $\beta(T)$ versus ρ_n is shown in figure 5. The relationship is reasonably linear for both sets of samples, implying that the pressure gradient should be more accurately given by

$$\nabla P = -(\eta_n/k)v_n - b_n\rho_n v_n^2. \qquad (14)$$

Equation (14) is the expected normal fluid contribution to the pressure gradient, and seems to imply that the superfluid contribution is negligable, if not non-existent. Values of b_n, based on equation (14), are included in Table 1, as are values of b_n determined in isothermal flow.[8] The two measurements agree fairly well.

While equation (14) implies that the parameter b_s is not measureable in this experiment, it turns out that it is still possible to estimate it. Isothermal flow measurements[6,8] from two separate experiments, using similar materials, indicate that a reasonable estimate is given by $b_n = 2b_s$. Even though this relationship has been tested to a very limited extent, it

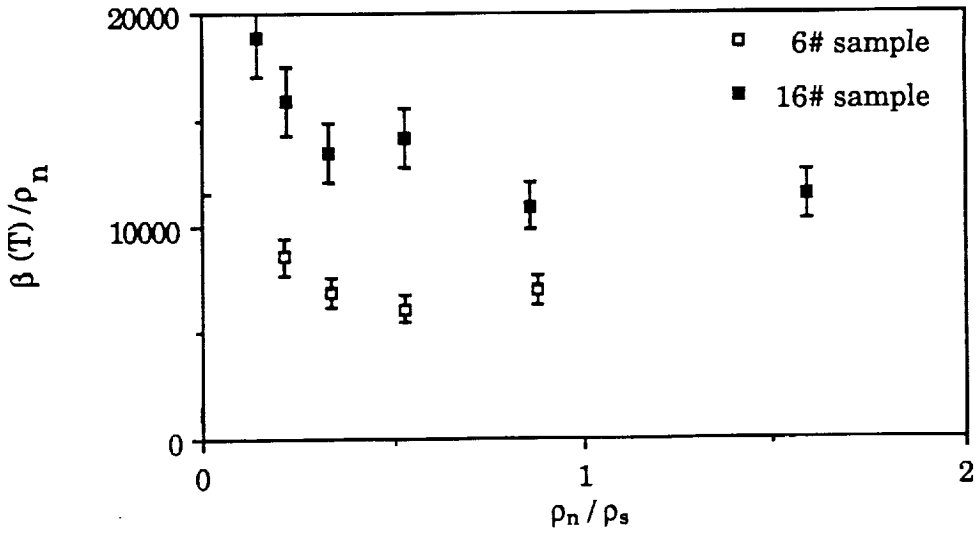

Figure 4 Temperature dependence of the quadratic coefficient $\beta(T)$ as given by equation (12).

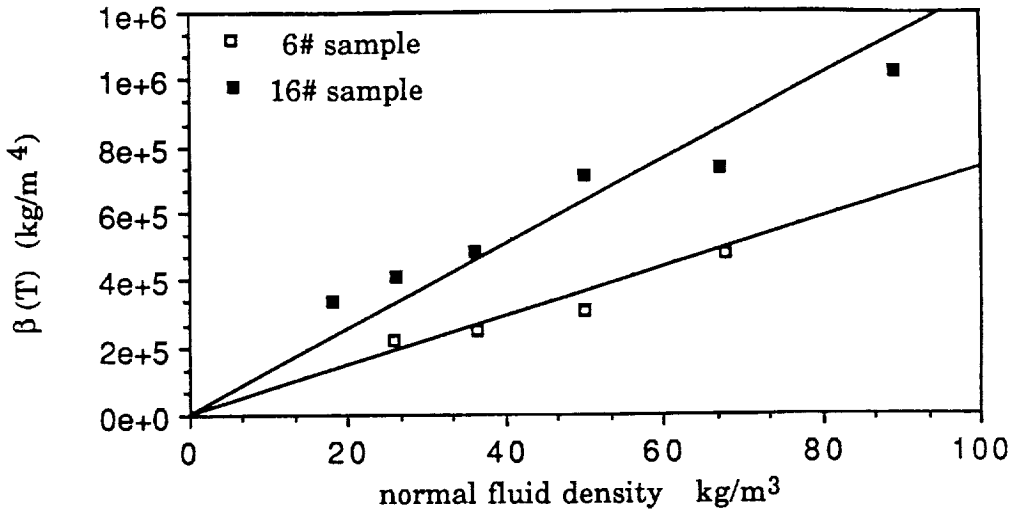

Figure 5 The temperature dependent, quadratic coefficient, β(T), as a function of rn only. The solid lines represent least square fits that have been forced through zero.

nonetheless makes it possible to obtain all the necessary parameters for calculating pressure drop from simple counterflow measurements.

When considering temperature data, the term F_s in equation (14) can, apparently, be ignored. However, the pressure gradient term is often less than one order of magnitude smaller than F_{sn}, so that, in general, it must be included. Equation (9) can be rearranged, then, to solve for F_{sn}, giving

$$\rho s \nabla T - \nabla P = A(T)\rho_n \rho (v_s - v_n)^3. \qquad (15)$$

Graphic solutions for A(T) are obtained from equation (15) by plotting the left hand side versus $(v_s - v_n)^3$. Values of A(T) as a function of temperature are plotted in figure 6, for both the 6# and 16# samples. The uncertainty in those values is on the order of ±100 m/s kg. For reference, a sample of the Gorter-Mellink coefficient for smooth tubes is included,[9] as well as A(T) calculated for the exit channels of the test section. The values of A(T) from the exit channels agree fairly well with the smooth tube results. In contrast, the values of A(T) for the porous samples are 2 to 4 times larger than smooth tube results, though the temperature dependence remains approximately the same. In addition, there appears to be some dependence on geometry.

Suprisingly, the 16# material shows less deviation from smooth tube results than does the 6# material. This result is opposite to what would be expected and remains unexplained. However, given the dramatic differences in geometry between porous media and smooth tubes, the relatively small variation of A(T) from smooth tube values of the Gorter-Mellink coefficient may imply that any geometry dependence of the parameter is very weak. In porous materials such as those considered in the present experiment, very large surface area to volume ratios and tortuous flow paths may give rise to inertial and path length effects.

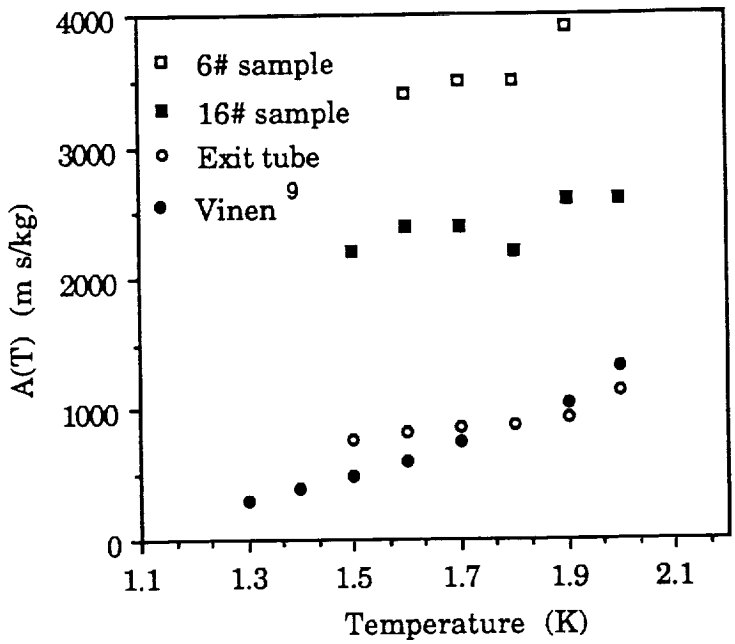

Figure 6 A plot of the Gorter-Mellink constant as a function of temperature, for both 6# and 16# samples

These effects may, in turn, account for why the parameter A(T) differs from measurements in smooth tubes.

CONCLUSIONS

The parameters necessary to estimate pressure and temperature gradients resulting from the flow of He II in high porosity ceramics can all be determined in counterflow. This approach offers a more accurate method of characterizing these materials for design purposes. Experimental results indicate that gradients can be predicted within 20%. Since counterflow experiments are relatively straightforward, it seems reasonable to suggest that they will provide a good and relatively easy characterization of any porous media.

ACKNOWLEDGEMENTS

Work supported in part by NASA/Goddard Space Flight Center under grant NAG-5-1031.

REFERENCES

1. M.J. DiPirro, Cryogenics, 30:193 (1990).
2. H. Rudiger and M. Wanner, Cryogenics, 27:38 (1987).
3. H. Nakai, and M. Murakami, Cryogenics, 27:442, (1987).
4. R. Srinivasan and A Hofmann, Cryogenics, 25:641, (1985).
5. G.L. Mills and A.R. Urbach, Cryogenics, 30:206, (1990).
6. J.R. Maddocks and S.W. Van Sciver, in: "Advances in Cryogenic engineering," Vol. 35A, Plenum Press, New York, (1990), p. 189
7. Lockheed Missles & Space Co. Inc., Astronautics Div. Sunnyvale, Ca.
8. J.R. Maddocks, "Transport Properties of He II flowing Through Porous Materials," PhD. Thesis, University of Wisconsin-Madison, Madison, Wisconsin (1991).
9. W.F. Vinen, Proc. Roy. Soc. (London), A240:114 (1957).